Met. Mater. Int., Vol. 19, No. 5 (2013), pp. 1041~1045
doi: 10.1007/s12540-013-5017-z

Properties and Pulsed Current Activated Consolidation of Nanostuctured $MgSiO_3$-$MgAl_2O_4$ Composites

In-Jin Shon[1,*], Song-Lee Du[1], Jung-Mann Doh[2], and Jin-Kook Yoon[2]

[1]Chonbuk National University, Division of Advanced Materials Engineering and the Research Center of Advanced Materials Development, Engineering College, Jeonju 561-756, Korea
[2]Korea Institute of Science and Technology, Interface Control Research Center, PO Box 131, Cheongryang, Seoul 130-650, Korea

(received date: 17 October 2012 / accepted date: 7 February 2013)

Nanocrystalline materials have received much attention as advanced engineering materials with improved physical and mechanical properties. As nanomaterials possess high strength, high hardness, excellent ductility and toughness, undoubtedly, more attention has been paid for the application of nanomaterials. Nanopowders of MgO, Al_2O_3 and SiO_2 were made by high energy ball milling. The simultaneous synthesis and consolidation of nanostuctured $MgAl_2O_4$-$MgSiO_3$ composites from milled 2MgO, Al_2O_3 and SiO_2 powders was investigated by the pulsed current activated sintering process. The advantage of this process is that it allows very quick densification to near theoretical density and inhibition of grain growth. Highly dense nanostructured $MgAl_2O_4$-$MgSiO_3$ composites were produced with a simultaneous application of 80 MPa pressure and a pulsed current of 2000A within 1 min. The fracture toughness of $MgAl_2O_4$-Mg_2SiO_4 composites sintered from 60 mol%MgO-20 mol%Al_2O_3-20 mol%SiO_2 powders milled for 4 h was 3.2 MPa·$m^{1/2}$. The fracture toughness of $MgAl_2O_4$-$MgSiO_3$ composite is higher than that of monolithic $MgAl_2O_4$.

Key words: sintering, $MgAl_2O_4$-$MgSiO_3$, composite, nanostructured material, powder metallurgy

1. INTRODUCTION

The attractive properties of $MgAl_2O_4$ are high hardness (16 GPa), low density (3.58 g/cm^3), high melting point (2135 °C), high chemical inertness, and high thermal shock resistance [1-3]. Because of its excellent properties, $MgAl_2O_4$ ceramic has been employed mainly in glass and steel industries, etc. However, as in the case of many ceramic materials, the current concern about these materials focuses on their low fracture toughness below the ductile-brittle transition temperature. To improve their mechanical properties, the approach commonly utilized has been the addition of a second phase to form composites and to make nanostructured materials.

Nanocrystalline materials have received much attention as advanced engineering materials with improved physical and mechanical properties [4,5]. As nanomaterials possess high strength and hardness, as well as excellent ductility and toughness, undoubtedly, more attention has been paid to the application of nanomaterials [6,7]. In recent days, nanocrystalline powders have been developed by the thermochemical and thermomechanical process named as the spray conversion process (SCP), co-precipitation and high energy milling [8-10]. The sintering temperature of high energy mechanically milled powder is lower than that of unmilled powder due to the increased reactivity, internal and surface energies, and surface area of the milled powder, which contribute to its so-called mechanical activation [11-13]. However, the grain size in sintered materials becomes much larger than that in pre-sintered powders due to rapid grain growth during a conventional sintering process. Therefore, even though the initial particle size is less than 100 nm, the grain size increases rapidly up to 2 μm or larger during conventional sintering [14]. So, controlling grain growth during the sintering process is one of the keys to the commercial success of nanostructured materials. In this regard, the pulsed current activated sintering method (PCASM), which can make dense materials within 2 min, has been shown to be effective in achieving this goal [15-17]. In addition, the spark plasma formed between the powder particles enhances the distorted energy of the particles and the rate of the diffusion between the particles [18-21].

In this study, we investigated the synthesis and sintering of $MgAl_2O_4$-$MgSiO_3$ composite by the PCAS method. The goal of this research is to produce dense nanostructured $MgAl_2O_4$-$MgSiO_3$ material. In addition, we also studied the microstructure and mechanical properties of $MgAl_2O_4$-$MgSiO_3$ composite.

*Corresponding author: ijshon@chonbuk.ac.kr

2. EXPERIMENTAL PROCEDURES

The Al_2O_3 powder with a grain size of <2.2 μm and 99.99% purity, amorphous SiO_2 powder with a grain size of < 100 μm and 99.8% purity, and MgO powder with a grain size of < 45 μm and 99% purity used in this research was supplied by Alfa. The powders (50 mol% MgO-25 mol%Al_2O_3-25 mol%SiO_2) were first milled in a high-energy ball mill (Pulverisette-5 planetary mill) at 250 rpm for 10 h. Tungsten carbide balls (10 mm in diameter) were used in a sealed cylindrical stainless steel vial under an argon atmosphere. The weight ratio of balls-to-powder was 30:1.

The powders were placed in a graphite die (outside diameter, 35 mm; inside diameter, 10 mm; height, 40 mm) and then introduced into the Pulsed Current Activated Sintering (PCAS) apparatus shown schematically in Fig. 1. The PCAS apparatus includes a 30 kW power supply which provides a pulsed current (on time; 20 μs, off time; 10 μs) through the sample, and 50 kN uniaxial press. The system was first evacuated and a uniaxial pressure of 80 MPa was applied. A pulsed current was then activated and maintained until the densification rate was negligible, as indicated by the real-time output of the shrinkage regarding the sample. The shrinkage was measured by a linear gauge measuring the vertical displacement. Temperatures were measured by a pyrometer focused on the surface of the graphite die. At the end of the process, the pulsed current was turned off and the sample cooled to room temperature. The process was carried out under a vacuum of 5.33 MPa.

Microstructural information was obtained from product samples, which had been polished and etched using thermal etching for 1 h at 1050 °C. Compositional and microstructural analyses of the products were made through X-ray diffraction (XRD), and field emission scanning electron microscopy (FE-SEM) with energy dispersive spectroscopy (EDS). Vickers hardness was measured by performing indentations at a load of 5 kg and a dwell time of 15 s. The grain sizes of the $MgSiO_3$ and $MgAl_2O_4$ was calculated from the full width at half-maximum (FWHM) of the diffraction peak by Suryanarayana and Grant Norton's formula [22].

$$B_r \cos\theta = (B_{crystalline} + B_{strain}) \cos\theta = k\lambda / L + \eta \sin\theta \quad (1)$$

where B_r is the full width at half-maximum (FWHM) of the diffraction peak after instrumental correction; $B_{crystalline}$ and B_{strain} are FWHM caused by small grain size and internal stress, respectively; k is constant (with a value of 0.9); λ is wavelength of the X-ray radiation; L and η are grain size and internal strain, respectively; and θ is the Bragg angle. The parameters B and B_r follow Cauchy's form with the relationship: $B = B_r + B_s$, where B and B_s are FWHM of the broadened Bragg peaks and the standard sample's Bragg peaks, respectively.

3. RESULTS AND DISCUSSION

Figure 2 illustrates the X-ray diffraction patterns of the 50 mol%MgO-25 mol%Al_2O_3-25 mol%SiO_2 powders after high-energy ball milling for 10 h. MgO and Al_2O_3 peaks are detected and SiO_2 peaks are not detected due to the amorphous phase. From the result, synthesis dose did not occur during the milling. FE-SEM images of 50 mol%MgO-25 mol%Al_2O_3-25 mol%SiO_2 powders with milling for 10 h are shown in Fig. 3. MgO, Al_2O_3 and SiO_2 powders have a round shape, refinement with milling and agglomeration. The variations of the shrinkage displacement and temperature with the heating time for the pulsed current of 2000 A during sintering of the high energy ball milled 50 mol%MgO-25 mol%Al_2O_3-25 mol%SiO_2 powders under a pressure of 80 MPa are shown in Fig. 3. The application of the pulsed current resulted in shrinkage due to consolidation. As pulsed

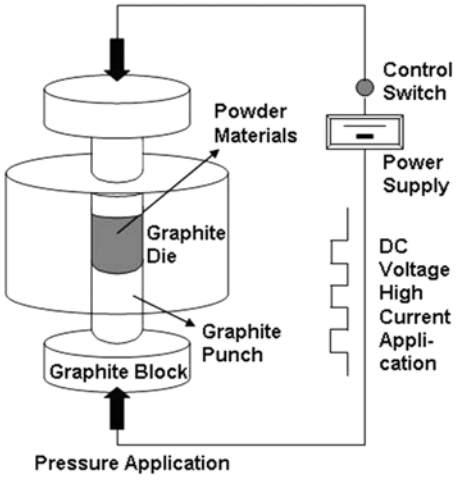

Fig. 1. Schematic diagram of apparatus for pulsed current activated sintering.

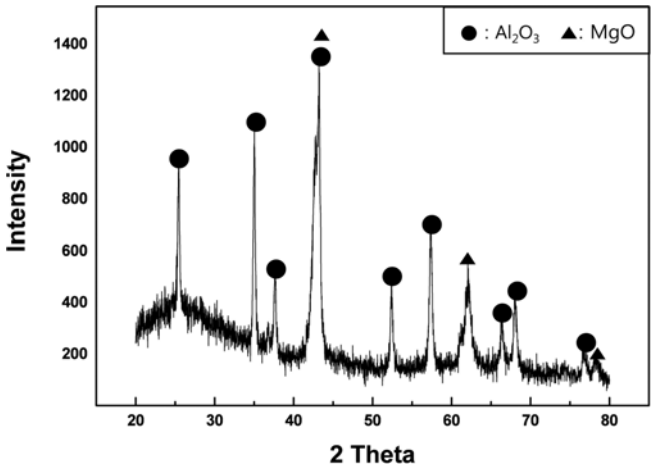

Fig. 2. X-ray diffraction pattern of the 50 mol%MgO-25 mol%Al_2O_3-25 mol%SiO_2 powder milled for 10 h.

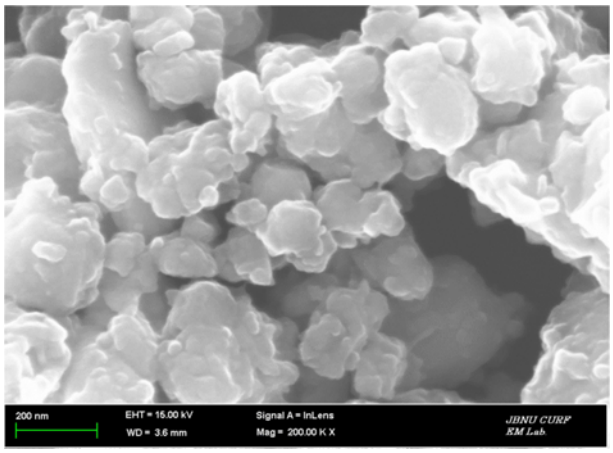

Fig. 3. FE-SEM image of the 50 mol%MgO-25 mol%Al_2O_3-25 mol%SiO_2 powders milled for 10 h.

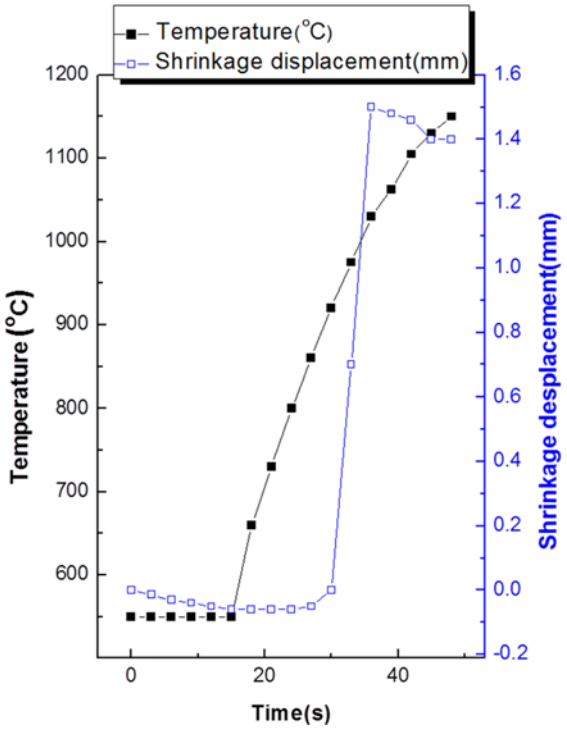

Fig. 4. Variations of temperature and shrinkage with heating time during the sintering of the 50 mol%MgO-25 mol%Al_2O_3-25 mol%SiO_2 powders milled for 10 h.

current was applied, the shrinkage displacement was nearly constant up to 900 ℃ and then increased abruptly. Figure 5 shows the XRD pattern of the specimen sintered to 1150 ℃ from the high energy ball milled 50 mol%MgO-25 mol%Al_2O_3-25 mol%SiO_2 powders. X-ray diffraction results, shown in Fig. 2 exhibit only peaks pertaining to the reactants MgO and Al_2O_3. However, when the temperature was raised to 1150 ℃, the starting powders reacted, producing highly dense products of $MgAl_2O_4$ and $MgSiO_3$. The interaction between these phases:

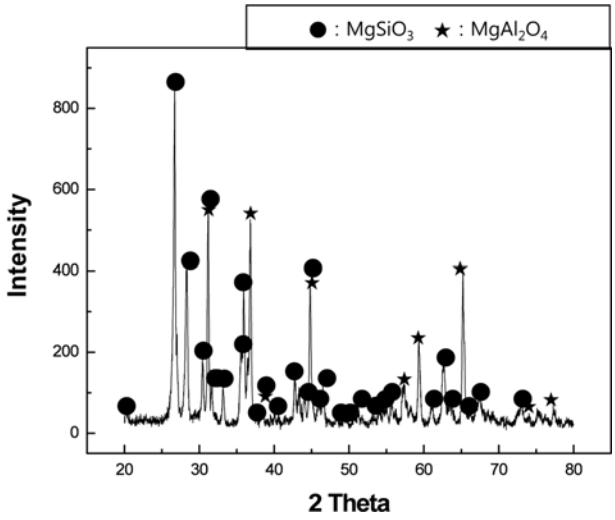

Fig. 5. X-ray diffraction pattern of the specimen sintered at 1150 ℃.

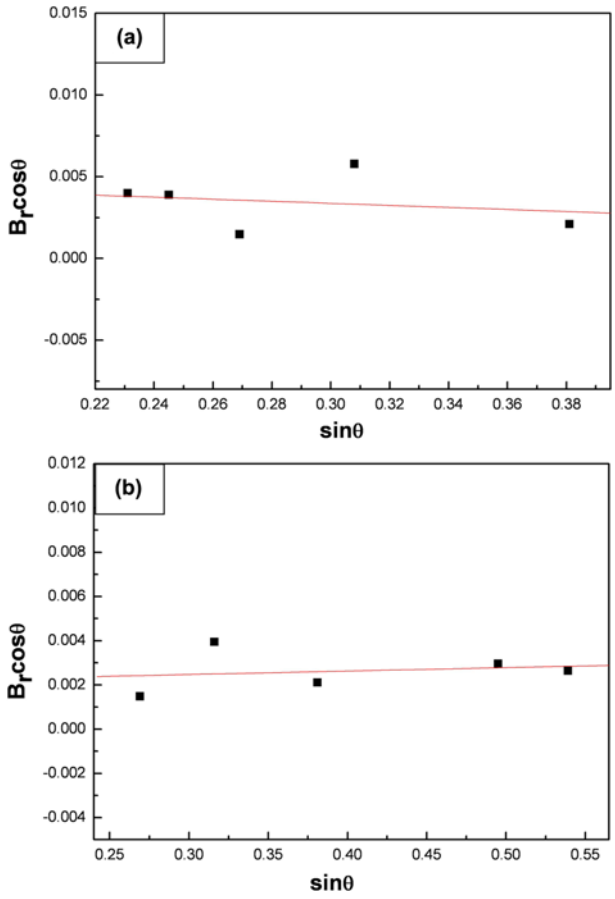

Fig. 6. Plot of B_r ($B_{crystalline}$+B_{strain}) cosθ versus sinθ for (a) $MgSiO_3$ and (b) $MgAl_2O_4$ in $MgAl_2O_4$-$MgSiO_3$ composite.

$$2MgO + Al_2O_3 + SiO_2 \rightarrow MgAl_2O_4 + MgSiO_3 \quad (2)$$

is thermodynamically feasible [23].

The abrupt increase in the displacement of shrinkage at the ignition temperature is due to the increase in density as a

result of the molar volume change associated with the formation of $MgAl_2O_4 + MgSiO_3$ from $2MgO + Al_2O_3 + SiO_2$ reactant and the consolidation of the product. Plot of B_r ($B_{crystalline} + B_{strain}$) $\cos\theta$ versus $\sin\theta$ in Suryanarayana and Grant Norton's formula [22] is shown in Fig. 6. The average grain sizes of the $MgAl_2O_4$ and $MgSiO_3$ in $MgAl_2O_4 + MgSiO_3$ composite calculated from the XRD data using Suryanarayana and Grant Norton's formula were approximately 69, 26 nm, respectively. Thus, the average grain size of the sintered $MgAl_2O_4$ and $MgSiO_3$ are not much larger than that of the initial powder, indicating the absence of great grain growth during sintering. This retention of the grain size is attributed to the high heating rate and the relatively short term exposure of the powders to high temperature. FE-SEM images of $MgAl_2O_4 + MgSiO_3$ composite sintered from 50 mol%MgO-25 mol%Al_2O_3-25 mol%SiO_2 powders milled for 10 h are shown in Fig. 7. $MgAl_2O_4$ and $MgSiO_3$ consist of nanocrystallines. In EDS, Al, Mg, Si and O peaks are detected and heavier contaminants, such as W and Fe from a ball or milling container, were not detected. The relative density of the product is about 99%.

The role of the current (resistive or inductive) in sintering and or synthesis has been the focus of several attempts aimed at providing an explanation to the observed enhancement of sintering and the improved characteristics of the products. The role played by the current has been variously interpreted,

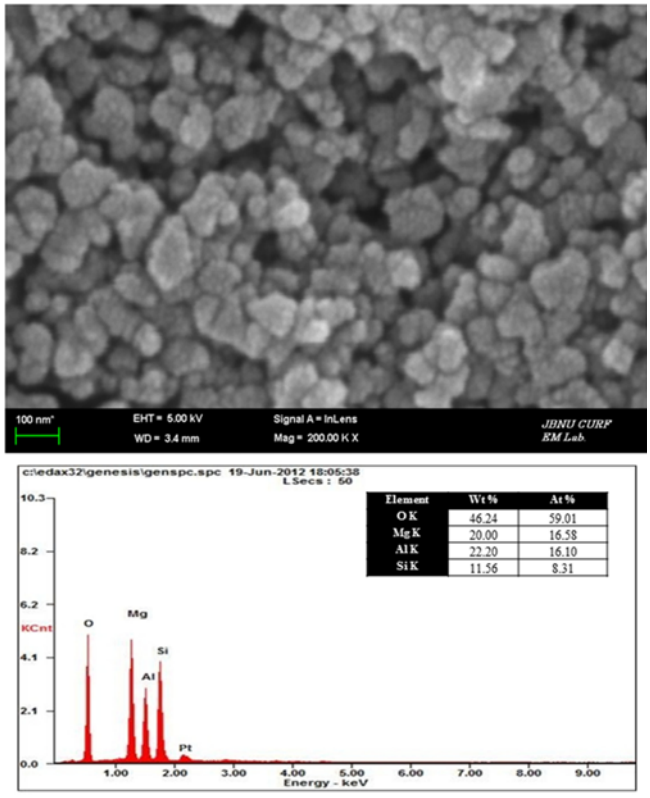

Fig. 7. FE-SEM image ans EDS of sintered $MgAl_2O_4$-$MgSiO_3$ composite.

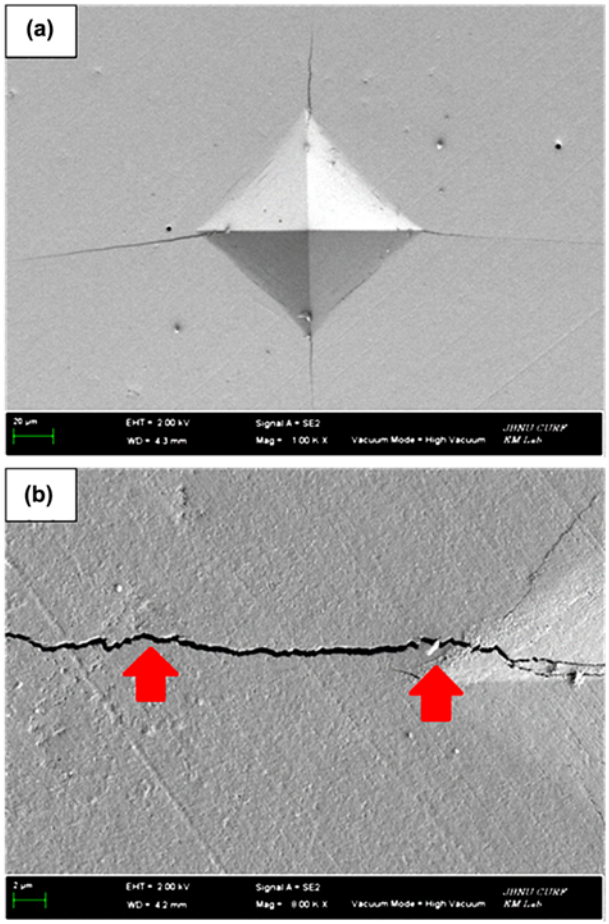

Fig. 8. (a) Vickers hardness indentation and (b) median crack propagation in the sintered $MgAl_2O_4$-$MgSiO_3$ composite.

the effect being explained in terms of the fast heating rate due to Joule heating, the presence of plasma in pores separating powder particles, and the intrinsic contribution of the current to mass transport [18-21].

Vickers hardness measurements were performed on polished sections of the $MgAl_2O_4 + Mg_2SiO_4$ composite using a 5 kg load and a dwell time of 15 s. The Vickers hardness's of $MgAl_2O_4 + MgSiO_3$ composite sintered from 50 mol%MgO-25 mol%Al_2O_3-25 mol%SiO_2 powders milled for 10 h was 780 kg/mm^2. Indentations with sufficient loads produced median cracks around the indent. The length of these cracks permits the estimation of the fracture toughness of the materials by means of the expression [24]:

$$K_{IC} = 0.203(c/a)^{-3/2} H_v \cdot a^{1/2} \quad (3)$$

where c is the trace length of the crack measured from the center of the indentation, a is one half of the average length of the two indent diagonals, and H_v is the hardness. The calculated fracture toughness value for the $MgAl_2O_4 + MgSiO_3$ composite sintered from 50 mol%MgO-25 mol%Al_2O_3-25 mol%SiO_2 powders is roughly 3.2 MPa·m$^{1/2}$. As in the case

of the hardness value, the toughness value is the average of five measurements. The fracture toughness of $MgAl_2O_4$ + $MgSiO_3$ composite is higher than that of monolithic $MgAl_2O_4$ because the crack can be blocked by $MgAl_2O_4$ and $MgSiO_3$, respectively [25]. A higher magnification view of an indentation median crack in the $MgAl_2O_4$ + $MgSiO_3$ composite is shown in Fig. 8(b), which shows that the crack propagated deflectively (↑).

4. CONCLUSIONS

Using the new rapid sintering method, PCAS, the densification of nanostuctured $MgAl_2O_4$-Mg_2SiO_4 composites was accomplished within 2 min from mechanically activated powders using high energy ball milling. The average grain sizes of the $MgAl_2O_4$ and Mg_2SiO_4 in $MgAl_2O_4$-Mg_2SiO_4 composites were approximately 60, 130 nm, respectively. The Vickers hardness and fracture toughness of $MgAl_2O_4$-Mg_2SiO_4 composites sintered from 60 mol%MgO-20 mol%Al_2O_3-20 mol%SiO_2 powders milled for 4 h were 1270 kg/mm^2 and 3.2 MPa·m$^{1/2}$, respectively. The hardness and fracture toughness of $MgAl_2O_4$-Mg_2SiO_4 composites were higher than monolithic Mg_2SiO_4.

ACKNOWLEGMENTS

This work is partially supported by KIST Future Resource Research Program and by the Human Resources Development of the Korea Institute of Energy Technology Evaluation and Planning (KETEP) grant funded by the Korea government Ministry of Knowledge Economy (No. 20114030200060).

REFERENCES

1. S. Anappan, L. J. Berchmans, and C. O. Augustin, *Mater. Lett*. **58**, 2283 (2004).
2. C. Baudin, R. Martinez, and P. Pena, *J. Am. Ceram. Soc*. **78**, 1857 (1995).
3. P. Hing, *J. Mater. Sci*. **11**, 1919 (1976).
4. M. Sherif El-Eskandarany, *J. Alloys Comd*. **305**, 225 (2000).
5. L. Fu, L. H. Cao, and Y. S. Fan, *Scripta Mater*. **44**, 1061 (2001).
6. K. Niihara, A. Nikahira, *Advanced Structural Inorganic Composite*, Elsevier Scientific Publishing Co., Trieste, Italy (1990).
7. S. Berger, R. Porat, and R. Rosen, *Progress in Materials* **42**, 311 (1997).
8. Z. Fang and J. W. Eason, *Int. J. of Refractory Met. & Hard Mater.* **13**, 297 (1995).
9. A. I. Y. Tok, L. H. Luo, and F. Y. C. Boey, *Mater. Sci. Eng. A* **383**, 229 (2004).
10. I. J. Shon, H. J. Wang, C. Y. Suh, S. W. Cho, and W. B. Kim, *Korean J. Met. Mater.* **49**, 374 (2011).
11. F. Charlot, E. Gaffet, B. Zeghmati, F. Bernard, and J. C. Liepce, *Mater. Sci. Eng. A* **262**, 279 (1999).
12. I. J. Shon, B. R. Kim, J. M. Doh, J. K. Yoon, and K. D. Woo, *J. Alloys Compd.* **489**, L4 (2010).
13. M. K. Beyer and H. Clausen-Schaumann, *Chem. Rev.* **105**, 2921 (2005).
14. J. Jung, S. Kang, *Scripta Mater*. **56**, 561 (2007).
15. S. L. Du, S. H. Cho, I. Y. Ko, J. M. Doh, J. K. Yoon, S. Y. Park, and I. J. Shon, *Korean J. Met. Mater.* **49**, 231 (2011).
16. H. S. Kang, I. Y. Ko, J. K. Yoon, J. M. Doh, K. T. Hong, and I. J. Shon, *Met. Mater. Int*. **17**, 57 (2011).
17. N. R. Park, I. Y. Ko, J. M. Doh, J. K. Yoon, and I. J. Shon, *Journal of Ceramic Processing Research* **12**, 660 (2011).
18. Z. Shen, M. Johnsson, Z. Zhao, and M. Nygren, *J. Am. Ceram. Soc*. **85**, 1921 (2002).
19. J. E. Garay, U. Anselmi-Tamburini, Z. A. Munir, S. C. Glade, and P. Asoka-Kumar, *Appl. Phys. Lett*. **85**, 573 (2004).
20. J. R. Friedman, J. E. Garay. U. Anselmi-Tamburini, and Z. A. Munir, *Intermetallics* **12**, 589 (2004).
21. J. E. Garay, J. E. Garay. U. Anselmi-Tamburini, and Z. A. Munir, *Acta Mater*. **51**, 4487 (2003).
22. C. Suryanarayana, M. Grant Norton, *X-ray Diffraction A Practical Approach*, Plenum Press, New York (1998).
23. O. Knacke, O. Kubaschewski, and K. Hesselmann, *Thermo Chemical Properties of Inorganic Substances*, p.1167, Springer-Verlag, New York (1991).
24. K. Niihara, R. Morena, and D. P. H. Hasselman, *J. Mater. Sci. Lett*. **1**, 12 (1982).
25. I. J. Shon, S. M. Kwak, J. M. Doh, B. J. Park, J. K. Yoon, *Res. Chem. Intermed*. (in press).